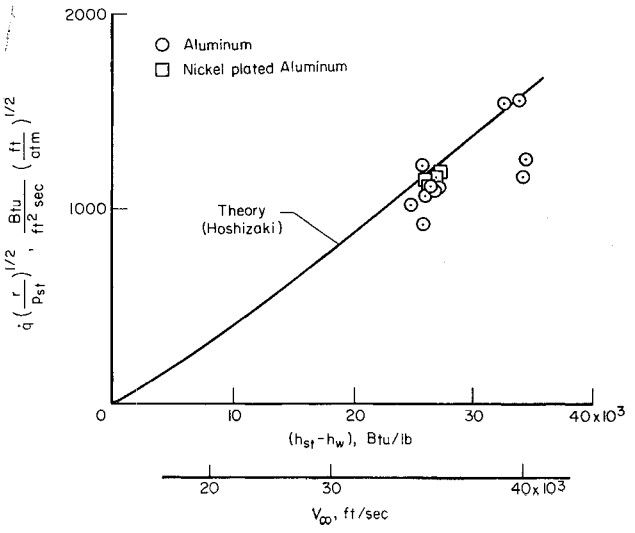

Fig. 1 Convective heating data.

into the wake where it produces a partially opaque screen visible on spark shadowgraphs. If the freestream density is adjusted correctly, melting can be made to begin during the portion of the model flight through the instrumented test section, and the time at which melting first occurs can be determined by studying successive shadowgraphs. From the melting-onset time the stagnation-point heating rate can be computed by solving the heat-conduction equation for the model interior. Although this technique is substantially different from the shock-tube technique, the stagnation conditions are nearly the same as those on stationary models in shock tubes at comparable enthalpy levels.

In order to study the effect of gage material, the surfaces of the aluminum models were nickel-electroplated. The thickness of the nickel coating was 0.0005 in., thick enough to assure a coherent nickel surface and thin enough so that, for purposes of solving the heat-conduction equation for the model interior, the nickel coat could be neglected. This was established from a solution of the heat-conduction equation for the composite model (assuming zero contact resistance between the nickel and aluminum), which showed that, over the flight trajectory, 97% of the heat transferred to the nickel surface reached the aluminum substrate. Thus, with respect to convective heat transfer, the model had the surface properties of nickel, and, with respect to conduction within the model, it had primarily the bulk properties of aluminum. Therefore, the convective heating-rate data from the present tests do not depend on the exact numerical values of density, specific heat, or temperature coefficient of resistivity for nickel.

Calibration tests of the nickel-plated aluminum models were performed in the same manner as for the uncoated aluminum models.[6] To wit, models were launched at a velocity at which ionization is negligible, 24,000 fps, and the time of melting onset was measured. Compared with the uncoated aluminum models, the nickel-plated models took a measurably longer time before melting was observed. This was partly because, as just described, the nickel shell absorbed a finite amount of heat, and partly because the shell had not reached melting temperature at the time when the aluminum substrate began to melt and apparently was not sluffed away immediately. The correction (applied to all data) for this effect, in terms of heating rate, was approximately 7% and should be nearly independent of test velocity since the heating rates at all test velocities were similar.

The results for the nickel-plated models at higher velocities are shown on Fig. 1 and are compared with similar data.[6] It is clear that, at a velocity of 36,000 fps, the heating rates are the same for both the aluminum and nickel-plated aluminum models. Furthermore, these heating rates are at the same general level as those measured with platinum gages[1-3] and platinum, nickel, and gold gages[5] and therefore, support the evidence that nickel gages do not lead to higher heating rates. Some additional data taken with aluminum models at a velocity of 41,000 fps are also shown on Fig. 1. All of these data agree reasonably well with the theory of Hoshizaki.[3]

References

[1] Gruszczynski, J. S. and Warren, W. R., Jr., "Experimental heat transfer studies of hypervelocity flight in planetary atmospheres," AIAA Paper 63–450 (1963).

[2] Rose, P. H. and Stankevics, J. O., "Stagnation point heat transfer measurements in partially ionized air," AIAA J. **1**, 2752–2763 (1963).

[3] Hoshizaki, H., "Heat transfer in planetary atmospheres at supersatellite speeds," ARS J. **32**, 1544–1551 (1962).

[4] Nerem, R. M., "Measurements of aerodynamic and radiative heating at super-orbital velocities," Ohio State Univ. Research Foundation Rept. 1598-1 (1964).

[5] Collins, D. J. and Spiegel, J. M., "Effect of gage material on convective heat transfer," AIAA J. **2**, 777–778 (1964).

[6] Compton, D. L. and Chapman, G. T., "Two new free-flight methods for obtaining convective-heat-transfer data," *AIAA Aerodynamic Testing Conference* (American Institute of Aeronautics and Astronautics, New York, 1964), pp. 115–128.

Aligned Magnetic Field Problem

S. Leibovich* and G. S. S. Ludford†
Cornell University, Ithaca, N. Y.

In a recent paper,[1] we considered the hydromagnetic flow engendered by a thin nonconducting airfoil set impulsively into motion in the direction of an applied magnetic field. The nonuniqueness in the steady problem was resolved by tracing the transient motion to its limit as time became infinite. The airfoil was assumed to be symmetric and the liquid perfectly conducting; only the slow-flow approximation was considered.

Figure 1 is a sketch of the magnetic field for Alfvén number $m = \frac{1}{3}$ according to this theory, which of course strictly applies for vanishingly small Alfvén numbers. Just enough magnetic lines are drawn into the airfoil from outside the current sheets to balance the flux across its surface. The main result is that finally the fluid between the two current sheets (thick lines) moves with the airfoil as if solid (slug flow), whereas outside the flow is undisturbed.

Since there are no magnetic sources inside the airfoil, there is no net magnetic force on it. On the other hand, continuity of total pressure requires a jump in dynamic pressure across the current sheets so that there is a pressure excess $\frac{1}{2}\mu[1 - (1 - m)^2]H_0^2$ at the front of the airfoil and a deficiency $\frac{1}{2}\mu[(1 + m)^2 - 1]H_0^2$ at the rear. These produce a drag

$$\tfrac{1}{2}\mu[(1 + m)^2 - (1 - m)^2]H_0^2 \cdot 2t = 4m\mu H_0^2 t$$

so that the drag coefficient, based on freestream dynamic pressure and chord, is $8\tau/m$, where τ is the thickness ratio.

Recently we were able to remove the restriction to slow flow and now have results for arbitrary sub-Alfvénic flow. The magnetic field is sketched in Fig. 2, which has two interesting aspects. First, the slow-flow figure is a remarkable approximation even for an Alfvén number as large as $\frac{1}{3}$. The influence of convection is to replace the singularities at the top and bottom of the profile by smooth current sheets;

Received August 4, 1964. This work has been supported by the Office of Naval Research under Contract No. Nonr-401(46).

* Research Assistant, Department of Theoretical and Applied Mechanics. Student Member AIAA.

† Professor of Applied Mathematics, Department of Theoretical and Applied Mechanics. Member AIAA.

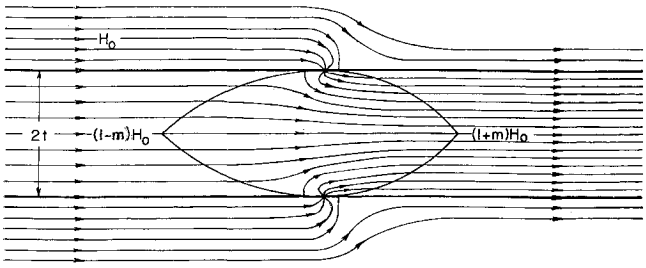

Fig. 1 The ultimate magnetic field for Alfvén number $m = \frac{1}{3}$ according to the slow-flow approximation. The vertical scale has been greatly enlarged.

no longer do magnetic lines from the outside fluid have to enter the airfoil. Secondly, features predicted by both Stewartson[2] and Sears-Resler[3] appear. The exterior flow pattern (i.e., outside the current sheets and following the magnetic lines) is a Sears-Resler potential flow over a portion of the airfoil at which there is a current sheet. However, the interior flow stemming from the remainder of the surface is a Stewartson slug flow.

The pressures between the current sheets are the same as before, but the rear pressure acts over a smaller area. Continuity of flux shows that the field under the current sheet on the body is $(1 - m)\ H_0/\alpha$, where $2\alpha t$ is the width of the airfoil at the point considered. This provides a pressure deficiency $\frac{1}{2}\mu[(1 - m)^2/\alpha^2 - 1]H_0^2$ at the body, so that the drag is now

$$\frac{1}{2}\mu(1 + m)^2H_0^2 \times 2\left(\frac{1 - m}{1 + m}\right)t + \frac{1}{2}\mu(1 - m)^2H_0^2 2t\int_{(1-m)/(1+m)}^{1}\frac{d\alpha}{\alpha^2} - \frac{1}{2}\mu(1 - m)^2H_0^2 \times 2t = 4m(1 - m)\mu H_0^2 t$$

and the drag coefficient is $8(1 - m)\tau/m$. The slow-flow theory overestimates the drag by a factor $1/(1 - m)$, which, in the case illustrated, is 1.5.

Details will be published shortly. Here it suffices to point out that quite novel methods are required. The perturbation within the current sheets is not small of the order of the thickness ratio, and the nonlinearity of the equations of motion must therefore be faced. This may be inferred from previous treatments of the problem, none of which attempts to do so. Fortunately the main disturbances are carried by slight modifications of Alfvén waves, which are exact solutions of the nonlinear equations.

Stewartson[4] has proposed that the following three limits be found in order to set the Sears-Resler solution[3] of the steady-state equations in its proper context: 1) vanishingly small misalignment, 2) conductivity tending to infinity, and 3) steady limit of transient solution. Our work provides the third limit and casts some doubt on whether the other two limits can be found by conventional perturbation schemes.

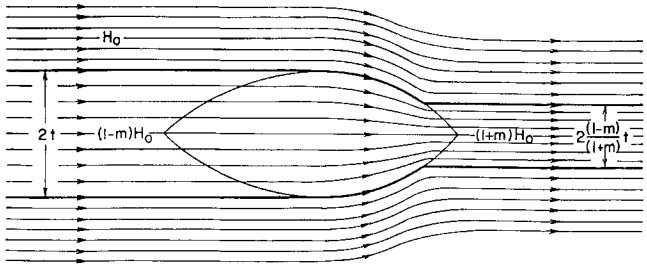

Fig. 2 The ultimate magnetic field for Alfvén number $m = \frac{1}{3}$ according to the nonlinear theory.

References

[1] Ludford, G. S. S. and Leibovich, S., "The ultimate hydromagnetic flow past an airfoil for an aligned magnetic field," Cornell Univ. TR 6, Office of Naval Research Contract Nonr-401(46); also Z. Angew. Math. Mech. (to be published).

[2] Stewartson, K., "On the motion of a non-conducting body through a perfectly conducting fluid," J. Fluid Mech. **8**, 82–96 (1960).

[3] Sears, W. R. and Resler, E. L., "Theory of thin airfoils in fluids of high electrical conductivity," J. Fluid. Mech. **5**, 257–273 (1959).

[4] Stewartson, K., "Magneto-fluid dynamics of bodies in aligned fields," Proc. Roy. Soc. (London) **A275**, 70–86 (1963).

One-Dimensional Flow in MHD Generators

EDGAR BENDOR*

Republic Aviation Corporation, Farmingdale, N. Y.

THE equations for the one-dimensional flow in Faraday-type MHD generators are readily solved for cases in which one of the flow variables is held constant. The solutions are well known and have been documented (for example, by Sutton[1]). But it does not appear to have been pointed out that these solutions are all particular cases of a more general solution, which follows immediately from the assumption that the ratio of loss of kinetic energy to loss of stagnation enthalpy is constant. Flows at constant velocity, constant pressure, etc., correspond to particular values of this ratio. The general solution is given here, and application of the results to closed power generation is briefly discussed.

A General Solution

The equations of momentum, energy, and state for a segmented electrode, Faraday-type generator, operating at constant load factor $K = E/vB$, are

$$\left.\begin{aligned} \rho v\frac{dv}{dx} + \frac{dp}{dx} + \sigma vB^2(1 - K) &= 0 \\ \rho\frac{d}{dx}\left(c_p t + \frac{1}{2}v^2\right) = -\sigma BE(1 - K) &= -K(1 - K)B^2\sigma v \\ p = (\gamma - 1)c_p\rho t/\gamma & \end{aligned}\right\} \quad (1)$$

where σ, E, B are the (scalar) conductivity and the electric and magnetic fields, respectively. P, p and T, t are the stagnation and static pressures and temperatures, and suffixes 1, 2 denote conditions at entry and exit from the uniform magnetic field. Other symbols have their usual significance. When these three equations are combined, one has

$$\gamma(1 - K)v\frac{dv}{dx} + c_p(K + \gamma - K\gamma)\frac{dt}{dx} + K(1 - \gamma)c_p t\frac{1}{\rho}\frac{d\rho}{dx} = 0 \quad (2)$$

In the absence of the heat losses, the output of the generator is given by the loss of total enthalpy. It is therefore convenient if H is chosen as the independent variable (particularly for application to closed cycle generator systems where optimizations are carried out in terms of total enthalpy ratios across components).

Received August 3, 1964.

* Specialist Research Engineer, Power Conversion Systems Division. Member AIAA.